CONVEX RELAXATIONS FOR QUADRATIC ON/OFF CONSTRAINTS AND APPLICATIONS TO OPTIMAL TRANSMISSION SWITCHING

KSENIA BESTUZHEVA*, HASSAN HIJAZI†,†, AND CARLETON COFFRIN‡

Abstract. This paper studies mixed-integer nonlinear programs featuring disjunctive constraints and trigonometric functions. We first characterize the convex hull of univariate quadratic on/off constraints in the space of original variables using perspective functions. We then introduce new tight quadratic relaxations for trigonometric functions featuring variables with asymmetrical bounds. These results are used to further tighten recent convex relaxations introduced for the Optimal Transmission Switching problem in Power Systems. Using the proposed improvements, along with aggressive bound propagation, we close 10 out of the 28 medium-size open test cases in the NESTA benchmark library. The tightened model has better computational results when compared to state-of-the-art formulations.

Key words. Mixed-Integer Nonlinear Programming, Perspective Relaxation, On/Off constraints, Optimal Transmission Switching, Trigonometric Functions

AMS subject classifications. 90C11, 90C26, 90C25, 90C30, 90C90

1. Introduction.

We study non-convex Mixed-Integer Nonlinear Programs of the form,

$$\text{(MINLP)} \qquad \begin{aligned} &\min \; f(\mathbf{x}, \mathbf{y}) \\ &\text{s.t.} \; g_i(\mathbf{x}, \mathbf{y}) \leqslant 0, \; \forall i \in I, \\ &\quad h_j(\mathbf{x}) \leqslant 0 \text{ if } z_j = 1, \; \forall j \in J, \\ &\quad \mathbf{x} \in \mathbb{R}^n, \mathbf{y} \in \mathbb{Z}^m. \end{aligned}$$

Functions f, g_i and h_j are assumed to be continuous and twice differentiable. Given a binary variable $z \in \{0, 1\}$, we are interested in the special case of a univariate quadratic on/off constraint,

$$\boldsymbol{a}x^2 + \boldsymbol{b}x + \boldsymbol{c} - y \leqslant 0, \text{ if } z = 1. \tag{1}$$

(1) is also known as a disjunctive or indicator constraint. We assume that the variable bounds are part of the disjunction, i.e.,

$$\begin{cases} \boldsymbol{x}^{l0} \leqslant x \leqslant \boldsymbol{x}^{u0}, \text{ if } z = 0, \\ \boldsymbol{x}^{l1} \leqslant x \leqslant \boldsymbol{x}^{u1}, \text{ if } z = 1. \end{cases}$$

In the optimization literature, on/off constraints are most oftenly formulated using the standard big-M approach [23],

$$\boldsymbol{a}x^2 + \boldsymbol{b}x - y \leqslant -\boldsymbol{c}z + \boldsymbol{M}(1 - z),$$

where $\boldsymbol{M}$ is a constant parameter guaranteeing that the constraint becomes redundant if $u = 0$. These big-M formulations often lead to weak continuous relaxations, and thus inefficient computational results.

*The Australian National University, Data61-CSIRO, Canberra 2601, Australia.
hassan.hijazi@anu.edu.au, ksenija.bestuzheva@data61.csiro.au
†Corresponding author.
‡Los Alamos National Laboratory, Los Alamos, New Mexico 87545.
cjc@lanl.gov

An alternative approach is to use disjunctive programming. Consider a general on/off constraint:

$$g(\mathbf{x}) \leqslant 0 \text{ if } z = 0,$$
$$\mathbf{x} \in \mathbb{R}^n, z \in \{0, 1\},$$
$$\mathbf{x}^l \leqslant \mathbf{x} \leqslant \mathbf{x}^u,$$

where $g(\mathbf{x}) : \mathbb{R}^n \to \mathbb{R}$ is a convex function, $\mathbf{x}^l$ and $\mathbf{x}^u$ are two vectors in $\mathbb{R}^n$. This constraint can be reformulated as a disjunction between two sets:

$$\begin{aligned} &\mathbf{x} \in \Gamma_0 \cup \Gamma_1, \\ (2) \qquad &\Gamma_0 = \{(\mathbf{x}, z) \in \mathbb{R}^n \times \{0, 1\} \mid z = 0,\ \mathbf{x}^l \leqslant \mathbf{x} \leqslant \mathbf{x}^u\}, \\ &\Gamma_1 = \{(\mathbf{x}, z) \in \mathbb{R}^n \times \{0, 1\} \mid z = 1,\ g(\mathbf{x}) \leqslant 0,\ \mathbf{x}^l \leqslant \mathbf{x} \leqslant \mathbf{x}^u\}. \end{aligned}$$

or, equivalently,

$$\begin{aligned} (3) \qquad &\mathbf{x} \in \text{conv}(\Gamma_0 \cup \Gamma_1), \\ &\mathbf{x} \in \mathbb{R}^n, z \in \{0, 1\} \end{aligned}$$

Dropping the integrality requirement on variable u results in a convex relaxation of (2) which is typically tighter than the big-M relaxation. The challenging task lies in finding a compact algebraic characterization of set (3), i.e., a representation defined in the space of original variables.

1.1. Related work. Extensive work has been done on deriving convex relaxations of on/off constraints defined in a higher-dimensional space. Stubbs and Mehrotra [29] have generalized the lifting procedure for linear sets [1, 22, 28] to the convex case. Ceria and Soares [7] have applied perspective functions to formulate the convex hull of a union of convex sets. Grossmann and Lee [14] used these results to describe the convex hull of a disjunction involving convex nonlinear inequalities. However, all these approaches require adding auxiliary variables to the original formulation, thus increasing the model size, and decreasing it computational efficiency.
Based on perspective functions, Günlük and Linderoth in [15] were able to propose a compact characterization of the convex hull when the set Γ_0 reduces to a single point. Hijazi et al [19] were able to generalize this result to cases where Γ_0 is a hyper-rectangle and the constraints are isotone. In a recent work, Belotti et al. [5] study the efficiency of non-convex formulations for on/off constraints in conjunction with aggressive bound tightening techniques. For a detailed literature review and additional results, we refer to the recent work by Bonami et al. in [6].
In this paper we extend the reach of relaxations based on perspective functions to non-monotone quadratic functions. In Section 2, we give the definition of a perspective function, review some results from disjunctive programming and provide the proof for our convex hull characterization. Quadratic relaxations of trigonometric functions are derived in Section 3. In Section 4, the Optimal Transmission Switching (OTS) problem in Energy Systems and its Quadratic Convex (QC) relaxation are presented. This problem is about finding an optimal configuration of a given power network where line switching is permitted. The new convex hull formulation is applied to the

non-monotone quadratic constraints in the QC relaxation, and other ways of strengthening the model are investigated. Finally, Section 5 reports the computational results and Section 6 concludes the paper.

2. The New Convex Hull.

2.1. Perspective functions. For a given convex function $f(\mathbf{x}) : \mathbb{R}^n \to \mathbb{R}$ its perspective function $\tilde{f} : \mathbb{R}^{n+1} \to (\mathbb{R} \cup \{+\infty\})$ is defined as:

$$\tilde{f} = (\mathbf{x}, z) = \begin{cases} zf(\mathbf{x}/z) \text{ if } z > 0 \\ +\infty \text{ otherwise.} \end{cases}$$

For each fixed $z = \boldsymbol{z}^0$ the function $\tilde{f}(\mathbf{x}, \boldsymbol{z}^0)$ represents a dilation of the original function $f(\mathbf{x})$.

A perspective function has a focal point, which is a point approached by the dilations as z approaches 0. By modifying the argument of the perspective function one can modify its focal point. We use this property to build our convex hulls.

Note that the perspective operator preserves convexity, i.e., if function f is convex, so will be its perspective $\tilde{f}$.

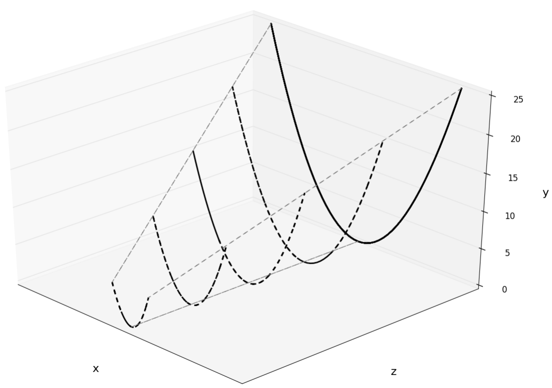

Fig. 1: Several dilations of the square function

2.2. State-of-the-art formulation. For completeness, we will re-state a result presented in [19], which characterizes the convex hull of a union of two convex sets defined by isotone functions.

Definition 1 ([19]). *Let $f : E \to \mathbb{R}, E \subseteq \mathbb{R}^n$.*

- *f is independently increasing (resp. decreasing) on coordinate i is for all $\mathbf{x} \in dom(f)$ and $\lambda > 0$ such that $\mathbf{x} + \lambda e_i \in dom(f)$, where e_i is ith unit vector of the standard basis, we have $f(\mathbf{x} + \lambda e_i) \geqslant f(\mathbf{x})$ (resp. $f(\mathbf{x} + \lambda e_i) \leqslant f(\mathbf{x})$).*
- *f is independently monotone on coordinate i if it is independently increasing or independently decreasing on the ith coordinate.*
- *f is isotone if it is independently monotone on every coordinate.*

Theorem 2 ([19]). *Let $f : E \to \mathbb{R}, E \subseteq \mathbb{R}^n$, be an isotone closed convex function with J^1 (resp., J^2) the set of indices on which f is independently increasing* *(resp. decreasing),*

$$\Gamma_0 = \{(\mathbf{x}, z) \in \mathbb{R}^n \times \{0,1\} \mid z = 0, \mathbf{l}^0 \leqslant \mathbf{x} \leqslant \mathbf{u}^0\},$$

$$\Gamma_1 = \{(\mathbf{x}, z) \in \mathbb{R}^n \times \{0,1\} \mid z = 1, f(\mathbf{x}) \leqslant 0, \mathbf{l}^1 \leqslant \mathbf{x} \leqslant \mathbf{u}^1\} \neq \varnothing,$$

Then $\operatorname{conv}(\Gamma_0 \cup \Gamma_1) = \operatorname{closure}(\Gamma')$, *where*

$$\Gamma'' = \left\{ \begin{array}{l} (\mathbf{x}, z) \in \mathbb{R}^{n+1} | \\ z q_S(\mathbf{x}, z) \leqslant 0 \quad \forall S \subset \{1, 2, ..., n\} \\ z l^1 + (1-z) l^0 \leqslant x \leqslant z u^1 + (1-z) u^0 \\ 0 < z \leqslant 1 \end{array} \right\},$$

$q_S = (f \circ h_S)$ *and* $h_S(\mathbb{R}^n \times [0,1] \to \mathbb{R}^n)$ *is defined by*

$$(h_S(\mathbf{x}, z))_i = \begin{cases} l_i^1 & \forall i \in S \cap J_1 \\ u_i^1 & \forall i \in S \cap J_2 \\ \frac{x_i - (1-z) u_i^0}{z} & \forall i \in J_1, \ i \notin S, \\ \frac{x_i - (1-z) l_i^0}{z} & \forall i \in J_2, \ i \notin S. \end{cases}$$

2.3. Convex hull of a non-monotone quadratic constraint. We start by proving the following lemma about convex hulls.

LEMMA 3. *Let* $D = D_1 \cup D_2$.

$$\textit{Then } \mathsf{conv}(D) = \mathsf{conv}(\mathsf{conv}(D_1) \cup \mathsf{conv}(D_2))$$

Proof. 1. $[\mathsf{conv}(D) \subseteq \mathsf{conv}(\mathsf{conv}(D_1) \cup \mathsf{conv}(D_2))]$
Since $D_1 \subseteq \mathsf{conv}(D_1)$ and $D_2 \subseteq \mathsf{conv}(D_2)$, we have that

$$D = D_1 \cup D_2 \subseteq \mathsf{conv}(D_1) \cup \mathsf{conv}(D_2).$$

By taking the convex hull of both sets we obtain that

$$\mathsf{conv}(D) \subseteq \mathsf{conv}(\mathsf{conv}(D_1) \cup \mathsf{conv}(D_2)).$$

2. $[\mathsf{conv}(\mathsf{conv}(D_1) \cup \mathsf{conv}(D_2)) \subseteq \mathsf{conv}(D)]$
Since $D_1 \subseteq D$ and $D_2 \subseteq D$, we have that

$$\mathsf{conv}(D_1) \subseteq \mathsf{conv}(D) \text{ and } \mathsf{conv}(D_2) \subseteq \mathsf{conv}(D),$$

leading to

$$(\mathsf{conv}(D_1) \cup \mathsf{conv}(D_2)) \subseteq \mathsf{conv}(D).$$

$\mathsf{conv}(\mathsf{conv}(D_1) \cup \mathsf{conv}(D_2))$ is the smallest convex set containing the union, and since $\mathsf{conv}(D)$ is a convex set containing the union, we can deduce that

$$\mathsf{conv}(\mathsf{conv}(D_1) \cup \mathsf{conv}(D_2)) \subseteq \mathsf{conv}(D).$$

□

Now, we shall prove our main result.

THEOREM 4. *Let* $f(x,y) = \boldsymbol{a}x^2 + \boldsymbol{b}x + \boldsymbol{c} - y,\ a > 0,$
$\Gamma_0 = \left\{(x,y,z) \in \mathbb{R}^2 \times \mathbb{B} \mid z = 0,\ \boldsymbol{x}^{l_0} \leqslant x \leqslant \boldsymbol{x}^{u_0},\ y = 0\right\}$, *and*
$\Gamma_1 = \left\{(x,y,z) \in \mathbb{R}^2 \times \mathbb{B} \;\middle|\; z = 1,\ \boldsymbol{x}^{l_1} \leqslant x \leqslant \boldsymbol{x}^{u_1},\ \boldsymbol{y}^l \leqslant y \leqslant \boldsymbol{y}^u,\ f(x,y) \leqslant 0\right\}$

$$\text{then } \mathsf{conv}(\Gamma_0 \cup \Gamma_1) =$$

$$\left\{ (x,y,z) \in \mathbb{R}^2 \times [0,1] \;\middle|\; \begin{array}{l} x - \boldsymbol{x}^{u_0}(1-z) + \boldsymbol{\rho} z \leqslant \sqrt{\frac{yz + \boldsymbol{\delta} z^2}{\boldsymbol{a}}}, \\ x - \boldsymbol{x}^{l_0}(1-z) + \boldsymbol{\rho} z \geqslant -\sqrt{\frac{yz + \boldsymbol{\delta} z^2}{\boldsymbol{a}}}, \\ \boldsymbol{x}^{u_1} + \boldsymbol{\rho} z \geqslant -\sqrt{\frac{yz + \boldsymbol{\delta} z^2}{\boldsymbol{a}}}, \\ \boldsymbol{x}^{l_1} + \boldsymbol{\rho} z \leqslant \sqrt{\frac{yz + \boldsymbol{\delta} z^2}{\boldsymbol{a}}}, \\ z\boldsymbol{x}^{l_1} + (1-z)\boldsymbol{x}^{l_0} \leqslant x \leqslant z\boldsymbol{x}^{u_1} + (1-z)\boldsymbol{x}^{u_0}, \\ \boldsymbol{y}^l z \leqslant y \leqslant \boldsymbol{y}^u z. \end{array} \right\}$$

where $\boldsymbol{\rho} = \frac{\boldsymbol{b}}{2\boldsymbol{a}}$ *and* $\boldsymbol{\delta} = \boldsymbol{\rho}^2 - \boldsymbol{c}$.

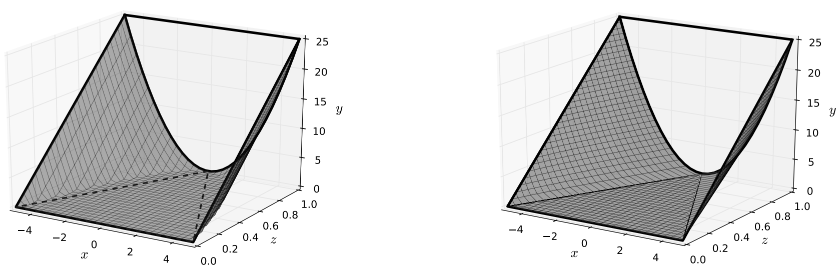

(a) Big-M formulation (b) Convex hull formulation

Fig. 2: Tightening convex relaxations

Proof. First, we split Γ_1 into

$$\Gamma_1^r = \{(x,y,z) \in \Gamma_0 \mid -\boldsymbol{\rho} \leqslant x \leqslant \boldsymbol{x}^{u_1}\}, \text{ and } \Gamma_1^l = \left\{(x,y,z) \in \Gamma_0 \mid \boldsymbol{x}^{l_1} \leqslant x \leqslant -\boldsymbol{\rho}\right\}.$$

Consider the set $\Gamma^r = \Gamma_0 \cup \Gamma_1^r$. For $x \in \Gamma_1^r$, f(x,y) is isotone, and its inverse can be taken. The inequality $f(x,y) \leqslant 0$ can be rewritten as:

$$\hat{f}(x,y) = x + \boldsymbol{\rho} - \sqrt{\frac{y + \boldsymbol{\delta}}{\boldsymbol{a}}} \leqslant 0$$

$\hat{f}(x,y)$ is isotone, thus Theorem 2 can be applied. Let us first construct the functions zq_S.

- $[S = \varnothing]$ $h_\varnothing(x,y,z) = \begin{pmatrix} (x-(1-z)\boldsymbol{x}^{u_0})/z \\ y/z \end{pmatrix}$,

$$zq_\varnothing = zf(h_\varnothing(x,y,z)) = x-(1-z)\boldsymbol{x}^{u_0} + \boldsymbol{\rho} z - \sqrt{\frac{yz+\boldsymbol{\delta} z^2}{\boldsymbol{a}}}.$$

- $[S = \{1\}]$ $h_1(x,y,z) = \begin{pmatrix} \boldsymbol{x}^{l_1} \\ y/z \end{pmatrix}$,

$$zq_1 = zf(h_1(x,y,z)) = \boldsymbol{x}^{l_1} + \boldsymbol{\rho} z - \sqrt{\frac{yz+\boldsymbol{\delta} z^2}{\boldsymbol{a}}}.$$

- $[S = \{2\}]$ $h_2(x,y,z) = \begin{pmatrix} (x-(1-z)\boldsymbol{x}^{u_0})/z \\ \boldsymbol{y}^u \end{pmatrix}$,

$$zq_2 = zf(h_2(x,y,z)) = x-(1-z)\boldsymbol{x}^{u_0} + \boldsymbol{\rho} z - \sqrt{\frac{\boldsymbol{y}^{u_1} z+z^2\boldsymbol{\delta}}{\boldsymbol{a}}}.$$

As $y \leqslant \boldsymbol{y}^{u_1}$, it is easy to see that the constraint $zq_2 \leqslant 0$ is dominated by $zq_\varnothing \leqslant 0$. Therefore, the convex hull is given by:

$$\mathsf{conv}(\Gamma^r) = \left\{ (x,y,z) \in \mathbb{R}^2 \times [0,1] \;\middle|\; \begin{array}{l} x - \boldsymbol{x}^{u_0}(1-z) + \boldsymbol{\rho} z \leqslant \sqrt{\frac{yz+\boldsymbol{\delta} z^2}{\boldsymbol{a}}}, \\ \boldsymbol{x}^{l_1} + \boldsymbol{\rho} z \leqslant \sqrt{\frac{yz+\boldsymbol{\delta} z^2}{\boldsymbol{a}}}, \\ -\boldsymbol{\rho} \leqslant x \leqslant z\boldsymbol{x}^{u_1} + (1-z)\boldsymbol{x}^{u_0}, \\ \boldsymbol{y}^l z \leqslant y \leqslant \boldsymbol{y}^u z. \end{array} \right\}$$

The convex hull of $\Gamma^l = \Gamma_0 \cup \Gamma_1^l$ can be obtained similarly:

$$\mathsf{conv}(\Gamma^l) = \left\{ (x,y,z) \in \mathbb{R}^2 \times [0,1] \;\middle|\; \begin{array}{l} x - \boldsymbol{x}^{l_0}(1-z) + \boldsymbol{\rho} z \geqslant -\sqrt{\frac{yz+\boldsymbol{\delta} z^2}{\boldsymbol{a}}}, \\ \boldsymbol{x}^{u_1} + \boldsymbol{\rho} z \geqslant -\sqrt{\frac{yz+\boldsymbol{\delta} z^2}{\boldsymbol{a}}}, \\ z\boldsymbol{x}^{l_1} + (1-z)\boldsymbol{x}^{l_0} \leqslant x \leqslant -\boldsymbol{\rho}, \\ \boldsymbol{y}^l z \leqslant y \leqslant \boldsymbol{y}^u z. \end{array} \right\}$$

Now we construct Γ' by taking a union of the two sets defined above: $\Gamma' = \mathsf{conv}(\Gamma^r) \cup \mathsf{conv}(\Gamma^l)$.

$$\Gamma' = \left\{ (x,y,z) \in \mathbb{R}^2 \times [0,1] \;\middle|\; \begin{array}{l} x - \boldsymbol{x}^{u_0}(1-z) + \boldsymbol{\rho} z \leqslant \sqrt{\frac{yz+\boldsymbol{\delta} z^2}{\boldsymbol{a}}} \\ \boldsymbol{x}^{l_1} + \boldsymbol{\rho} z \leqslant \sqrt{\frac{yz+\boldsymbol{\delta} z^2}{\boldsymbol{a}}} \\ x - \boldsymbol{x}^{l_0}(1-z) + \frac{\boldsymbol{b}u}{2\boldsymbol{a}} \geqslant -\sqrt{\frac{yz+\boldsymbol{\delta} z^2}{\boldsymbol{a}}} \\ \boldsymbol{x}^{u_1} + \boldsymbol{\rho} z \geqslant -\sqrt{\frac{yz+\boldsymbol{\delta} z^2}{\boldsymbol{a}}} \\ z\boldsymbol{x}^{l_1} + (1-z)\boldsymbol{x}^{l_0} \leqslant x \leqslant z\boldsymbol{x}^{u_1} + (1-z)\boldsymbol{x}^{u_0} \\ \boldsymbol{y}^l z \leqslant y \leqslant \boldsymbol{y}^u z. \end{array} \right\}$$

We have that $\Gamma_0 \cup \Gamma_1 = \Gamma^r \cup \Gamma^l$ by definition of these sets. From Lemma 3 we have that $\mathsf{conv}(\Gamma^r \cup \Gamma^l) = \mathsf{conv}(\mathsf{conv}(\Gamma^r) \cup \mathsf{conv}(\Gamma^l)) = \mathsf{conv}(\Gamma')$. It is easy to see that Γ' is convex, thus $\mathsf{conv}(\Gamma^r \cup \Gamma^l) = \Gamma'$.

∎

Figure 2 compares the convex hull to the region defined by the big-M constraint.

3. Quadratic Outer Approximations of Trigonometric Functions. In this section, we derive quadratic relaxations for trigonometric functions $f(x)$, $\boldsymbol{x}^l \leqslant x \leqslant \boldsymbol{x}^u$, and we consider the case $(\boldsymbol{x}^u - \boldsymbol{x}^l) < \pi/2$, with asymmetrical bounds. To the best of our knowledge, this is the first quadratic relaxation of trigonometric functions exploiting asymmetrical bounds on x.

Let $Q_f(\boldsymbol{x}_1, \boldsymbol{x}_2, \boldsymbol{x}_3)$ denote the equation of the quadratic function passing through three distinct points $(\boldsymbol{x}_1; f(\boldsymbol{x}_1)), (\boldsymbol{x}_2; f(\boldsymbol{x}_2))$, and $(\boldsymbol{x}_3; f(\boldsymbol{x}_3))$.

$$Q_f(\boldsymbol{x}_1, \boldsymbol{x}_2, \boldsymbol{x}_3) = \frac{\boldsymbol{\phi}_{32}\boldsymbol{\delta}_{21} - \boldsymbol{\phi}_{21}\boldsymbol{\delta}_{32}}{\boldsymbol{\delta}_{21}\boldsymbol{\delta}_{31}\boldsymbol{\delta}_{32}}(x - \boldsymbol{x}_1)(x - \boldsymbol{x}_2) + \frac{\boldsymbol{\phi}_{21}}{\boldsymbol{\delta}_{21}}(x - \boldsymbol{x}_2) + f(\boldsymbol{x}_2)$$

where $\boldsymbol{\delta}_{ij} = \boldsymbol{x}_i - \boldsymbol{x}_j$ and $\boldsymbol{\phi}_{ij} = f(\boldsymbol{x}_i) - f(\boldsymbol{x}_j)$.

PROPOSITION 5. *Given* ϵ *s.t.* $0 < \epsilon < \frac{\pi}{2} - \boldsymbol{x}^u$, *if* $0 \leqslant \boldsymbol{x}^l \leqslant \boldsymbol{x}^u < \frac{\pi}{2}$, *then*

$$\cos(\boldsymbol{x}^u + \epsilon) \leqslant \cos(\boldsymbol{x}^u) - \epsilon \sin(\boldsymbol{x}^u)$$

Proof. Consider the tangent to the function $\cos(x)$ at $x = \boldsymbol{x}^u$. Its equation is written $f(x) = \cos(\boldsymbol{x}^u) - \sin(\boldsymbol{x}^u)(x - \boldsymbol{x}^u)$. It lies above the cosine function since $\cos(x)$ is concave for $0 < x < \frac{\pi}{2}$. Then for all $0 \leqslant \epsilon \leqslant \frac{\pi}{2} - \boldsymbol{x}^u$ we have:

$$\cos(\boldsymbol{x}^u + \epsilon) \leqslant f(\boldsymbol{x}^u + \epsilon) = \cos(\boldsymbol{x}^u) - \epsilon \sin(\boldsymbol{x}^u)$$

∎

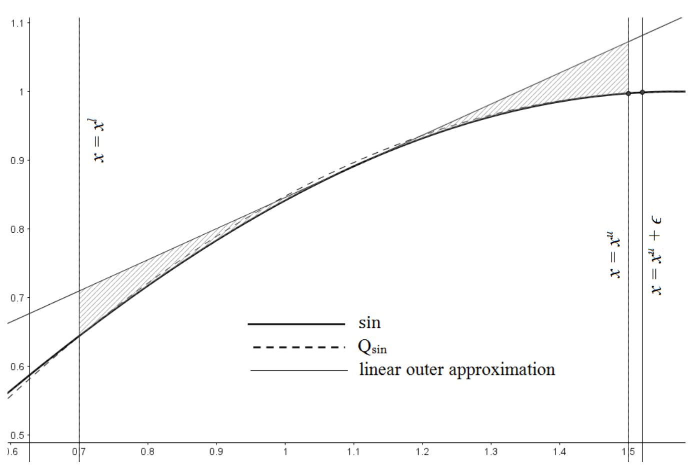

Fig. 3: For the sine function, we compare a linear outer approximation to the new quadratic relaxation defined by the points $(\boldsymbol{x}^l; \sin(\boldsymbol{x}^l)), (\boldsymbol{x}^u; \sin(\boldsymbol{x}^u))$, and $(\boldsymbol{x}^u + \epsilon; \sin(\boldsymbol{x}^u + \epsilon))$

THEOREM 6. *Given* ϵ *s.t.* $0 < \epsilon < \frac{\pi}{2} - \boldsymbol{x}^u$, *if* $0 \leqslant \boldsymbol{x}^l \leqslant \boldsymbol{x}^u < \frac{\pi}{2}$, *then*

$$\sin(x) \leqslant Q_{\sin}(\boldsymbol{x}^l, \boldsymbol{x}^u, \boldsymbol{x}^u + \epsilon), \ \forall x \in [\boldsymbol{x}^l, \boldsymbol{x}^u].$$

Proof. We have $\boldsymbol{x}_1 = \boldsymbol{x}^l, \boldsymbol{x}_2 = \boldsymbol{x}^u$ and $\boldsymbol{x}_3 = \boldsymbol{x}^u + \epsilon$. This leads to $\boldsymbol{\delta}_{32} = \boldsymbol{x}_u + \epsilon - \boldsymbol{x}_u = \epsilon$ and $\boldsymbol{\delta}_{31} = (\boldsymbol{x}_u + \epsilon) - \boldsymbol{x}_l = \boldsymbol{\delta}_{21} + \epsilon$. Consider the function corresponding to the difference between $Q_{\sin}()$ and $\sin()$,

$$\begin{aligned} f_\epsilon(x) &= Q_{\sin}(\boldsymbol{x}^l, \boldsymbol{x}^u, \boldsymbol{x}^u + \epsilon) - \sin(x) \\ &= \frac{\boldsymbol{\phi}_{32}\boldsymbol{\delta}_{21} - \boldsymbol{\phi}_{21}\epsilon}{\boldsymbol{\delta}_{21}^2\epsilon + \boldsymbol{\delta}_{21}\epsilon^2}(x - \boldsymbol{x}_1)(x - \boldsymbol{x}_2) + \frac{\boldsymbol{\phi}_{21}}{\boldsymbol{\delta}_{21}}(x - \boldsymbol{x}_2) + \sin(\boldsymbol{x}_2) - \sin(x) \end{aligned}$$

We will first show that $f_\epsilon(x)$ is strictly decreasing at $\boldsymbol{x}^u$. Since $f_\epsilon(\boldsymbol{x}^u) = 0$, this implies that f is positive in the neighborhood below $\boldsymbol{x}^u$. We will then show that $f_\epsilon(x)$ has a unique stationary point in the interval $[\boldsymbol{x}^l, \boldsymbol{x}^u]$. Since $f_\epsilon(\boldsymbol{x}^l) = f_\epsilon(\boldsymbol{x}^u) = 0$, this is sufficient to prove that $f_\epsilon(x)$ is positive on the hole interval.
Let us consider the derivative of $f_\epsilon(x)$,

$$f_\epsilon^{'}(x) = \frac{\boldsymbol{\phi}_{32}\boldsymbol{\delta}_{21} - \boldsymbol{\phi}_{21}\epsilon}{\boldsymbol{\delta}_{21}^2\epsilon + \boldsymbol{\delta}_{21}\epsilon^2}(2x - \boldsymbol{x}_1 - \boldsymbol{x}_2) + \frac{\boldsymbol{\phi}_{21}}{\boldsymbol{\delta}_{21}} - \cos(x)$$

Now consider $f_\epsilon^{'}(\boldsymbol{x}^u) = f_\epsilon^{'}(\boldsymbol{x}_2)$,

$$\begin{aligned} f_\epsilon^{'}(\boldsymbol{x}_2) &= \frac{\boldsymbol{\phi}_{32}\boldsymbol{\delta}_{21} - \boldsymbol{\phi}_{21}\epsilon}{\boldsymbol{\delta}_{21}^2\epsilon + \boldsymbol{\delta}_{21}\epsilon^2}(2\boldsymbol{x}_2 - \boldsymbol{x}_1 - \boldsymbol{x}_2) + \frac{\boldsymbol{\phi}_{21}}{\boldsymbol{\delta}_{21}} - \cos(\boldsymbol{x}_2) \\ &= \frac{\boldsymbol{\phi}_{32}\boldsymbol{\delta}_{21} - \boldsymbol{\phi}_{21}\epsilon}{\boldsymbol{\delta}_{21}^2\epsilon + \boldsymbol{\delta}_{21}\epsilon^2}(\boldsymbol{x}_2 - \boldsymbol{x}_1) + \frac{\boldsymbol{\phi}_{21}}{\boldsymbol{\delta}_{21}} - \cos(\boldsymbol{x}_2) \\ &= \frac{\boldsymbol{\phi}_{32}\boldsymbol{\delta}_{21} - \boldsymbol{\phi}_{21}\epsilon}{\boldsymbol{\delta}_{21}^2\epsilon + \boldsymbol{\delta}_{21}\epsilon^2}\boldsymbol{\delta}_{21} + \frac{\boldsymbol{\phi}_{21}}{\boldsymbol{\delta}_{21}} - \cos(\boldsymbol{x}_2) \\ &= \frac{\boldsymbol{\phi}_{32}\boldsymbol{\delta}_{21} - \boldsymbol{\phi}_{21}\epsilon}{\epsilon(\boldsymbol{\delta}_{21} + \epsilon)} + \frac{\boldsymbol{\phi}_{21}}{\boldsymbol{\delta}_{21}} - \cos(\boldsymbol{x}_2) \\ &= \frac{\boldsymbol{\phi}_{32}\boldsymbol{\delta}_{21}}{\epsilon(\boldsymbol{\delta}_{21} + \epsilon)} - \frac{\boldsymbol{\phi}_{21}}{\boldsymbol{\delta}_{21} + \epsilon} + \frac{\boldsymbol{\phi}_{21}}{\boldsymbol{\delta}_{21}} - \cos(\boldsymbol{x}_2) \\ &= \frac{\boldsymbol{\phi}_{32}\boldsymbol{\delta}_{21} - \epsilon\boldsymbol{\phi}_{21} + \epsilon(\boldsymbol{\delta}_{21} + \epsilon)\left(\frac{\boldsymbol{\phi}_{21}}{\boldsymbol{\delta}_{21}} - \cos(\boldsymbol{x}_2)\right)}{\epsilon(\boldsymbol{\delta}_{21} + \epsilon)} = \frac{h(\epsilon)}{\epsilon(\boldsymbol{\delta}_{21} + \epsilon)}, \end{aligned}$$

where

$$h(\epsilon) = \boldsymbol{\phi}_{32}\boldsymbol{\delta}_{21} - \epsilon\boldsymbol{\phi}_{21} + \epsilon(\boldsymbol{\delta}_{21} + \epsilon)\left(\frac{\boldsymbol{\phi}_{21}}{\boldsymbol{\delta}_{21}} - \cos(\boldsymbol{x}_2)\right)$$

Since $\epsilon(\boldsymbol{\delta}_{21} + \epsilon) > 0$, we have that $f_\epsilon^{'}(\boldsymbol{x}_2) \leqslant 0 \Leftrightarrow h'(\epsilon) \leqslant 0$.
Consider the derivative of h,

$$\begin{aligned} h'(\epsilon) &= \boldsymbol{\delta}_{21}\cos(\boldsymbol{x}_2 + \epsilon) - \boldsymbol{\phi}_{21} + (\boldsymbol{\delta}_{21} + 2\epsilon)\left(\frac{\boldsymbol{\phi}_{21}}{\boldsymbol{\delta}_{21}} - \cos(\boldsymbol{x}_2)\right) \\ &= \boldsymbol{\delta}_{21}\left(\cos(\boldsymbol{x}_2 + \epsilon) - \cos(\boldsymbol{x}_2)\right) + 2\epsilon\left(\frac{\boldsymbol{\phi}_{21}}{\boldsymbol{\delta}_{21}} - \cos(\boldsymbol{x}_2)\right) \end{aligned}$$

Based on Proposition 5, we have that $\cos(\boldsymbol{x}_2 + \epsilon) - \cos(\boldsymbol{x}_2) \leqslant \epsilon\sin(\boldsymbol{x}_2)$, consequently,

$$\begin{aligned} h'(\epsilon) &\leqslant -\epsilon\boldsymbol{\delta}_{21}\sin(\boldsymbol{x}_2) + 2\epsilon\left(\frac{\boldsymbol{\phi}_{21}}{\boldsymbol{\delta}_{21}} - \cos(\boldsymbol{x}_2)\right) \\ &\leqslant \epsilon\left(2\frac{\boldsymbol{\phi}_{21}}{\boldsymbol{\delta}_{21}} - 2\cos(\boldsymbol{x}_2) - \boldsymbol{\delta}_{21}\sin(\boldsymbol{x}_2)\right) \end{aligned}$$

We will next to show that

$$2\frac{\boldsymbol{\phi}_{21}}{\boldsymbol{\delta}_{21}} - 2\cos(\boldsymbol{x}_2) - \boldsymbol{\delta}_{21}\sin(\boldsymbol{x}_2) \leqslant 0$$

or, equivalently,

$$\begin{aligned} g(\boldsymbol{\delta}_{21}) &= \boldsymbol{\phi}_{21} - \boldsymbol{\delta}_{21}\cos(\boldsymbol{x}_2) - \frac{1}{2}\boldsymbol{\delta}_{21}^2\sin(\boldsymbol{x}_2) \\ &= \sin(\boldsymbol{x}_2) - \sin(\boldsymbol{x}_2 - \boldsymbol{\delta}_{21}) - \boldsymbol{\delta}_{21}\cos(\boldsymbol{x}_2) - \frac{1}{2}\boldsymbol{\delta}_{21}^2\sin(\boldsymbol{x}_2) \leqslant 0 \end{aligned}$$

Consider the derivatives:

$$g'(\boldsymbol{\delta}_{21}) = \cos(\boldsymbol{x}_2 - \boldsymbol{\delta}_{21}) - \cos(\boldsymbol{x}_2) - \boldsymbol{\delta}_{21}\sin(\boldsymbol{x}_2)$$

$$g''(\boldsymbol{\delta}_{21}) = \sin(\boldsymbol{x}_2 - \boldsymbol{\delta}_{21}) - \sin(\boldsymbol{x}_2) < 0$$

Since $g(0) = 0$, $g'(0) = 0$ and $g''(\boldsymbol{\delta}_{21}) < 0$, we have proved that $g(\boldsymbol{\delta}_{21}) \leqslant 0,\ \forall \boldsymbol{\delta}_{21} \geqslant 0$ and thus $f_\epsilon^{'}(\boldsymbol{x}_2) \leqslant 0,\ \forall\epsilon,\ 0 < \epsilon < \frac{\pi}{2} - \boldsymbol{x}^u$. Since $f_\epsilon^{'}(x)$ is a convex function and is negative at the upper bound $\boldsymbol{x}^u$, it can have at most one root in the interval $[\boldsymbol{x}^l, \boldsymbol{x}^u]$. Consequently f_ϵ has a unique stationary point in this interval. Since $f_\epsilon(\boldsymbol{x}^l) = f_\epsilon(\boldsymbol{x}^u) = 0$, and f_ϵ is positive in the neighborhood of $\boldsymbol{x}^y$, it is positive on the hole interval.

□

Note that this proof can be easily adapted to the case $f(x) = \cos(x),\ x \in [-\pi/2, 0]$ by translating the x axis by $\pi/2$. It can also be adapted to $\cos(x),\ x \in [0, \pi/2]$ and $\sin(x),\ x \in [-\pi/2, 0]$ by inverting the sign of x.
Having a quadratic relaxation for $\sin(x)$ and $\cos(x)$ enables us to use the convex-hull formulation of quadratic on/off constraints introduced in Section 2.

4. Optimal Transmission Switching.

The Optimal Transmission Switching (OTS) problem is an extension of the Optimal Power Flow (OPF) problem where power lines can be switched on/off.

4.1. The Optimal Power Flow (OPF) problem.

We consider a network $\langle N, E\rangle$, where N is the set of buses (nodes) and E is the set of lines (edges) linking pairs of nodes in both directions. Each bus has two variables: a voltage magnitude v_i, and a phase angle θ_i. The physical properties of the lines are described by two constants, the susceptance $\mathbf{b}_{ij}$, and the conductance $\mathbf{g}_{ij}$. The AC power flows in the network are defined by

$$\begin{aligned} p_{ij} &= \mathbf{g}_{ij}v_i^2 - \mathbf{g}_{ij}v_iv_j\cos(\theta_{ij}) - \mathbf{b}_{ij}v_iv_j\sin(\theta_{ij}) \quad \forall (i,j) \in E \\ q_{ij} &= -\mathbf{b}_{ij}v_i^2 + \mathbf{b}_{ij}v_iv_j\cos(\theta_{ij}) - \mathbf{g}_{ij}v_iv_j\sin(\theta_{ij}) \quad \forall (i,j) \in E \end{aligned} \tag{4}$$

where p_{ij} and q_{ij} represent respectively active and reactive power flowing through line $(i, j) \in E$, and $\theta_{ij} = \theta_i - \theta_j$ is the voltage angle difference. Another physical constraint in the network is Kirchhoff's Current Law, where p_i^g and q_i^g respectively denote active and reactive power generation, and $\mathbf{p}_i^l$ and $\mathbf{q}_i^l$ are constant predefined loads at bus i:

$$\begin{aligned} p_i^g - \mathbf{p}_i^l &= \sum_{(i,j)\in E} p_{ij} \quad \forall i \in N \\ q_i^g - \mathbf{q}_i^l &= \sum_{(i,j)\in E} q_{ij} \quad \forall i \in N \end{aligned} \tag{5}$$

The operational constraints in the network are the following:

$$\boldsymbol{p}_i^{gl} \leqslant p_i^g \leqslant \boldsymbol{p}_i^{gu} \quad \forall i \in N \tag{6a}$$

$$\boldsymbol{q}_i^{gl} \leqslant q_i^g \leqslant \boldsymbol{q}_i^{gu} \quad \forall i \in N \tag{6b}$$

$$\boldsymbol{v}_i^{l} \leqslant v_i \leqslant \boldsymbol{v}_i^{u} \quad \forall i \in N \tag{6c}$$

$$\boldsymbol{\theta}_{ij}^{l} \leqslant \theta_{ij} \leqslant \boldsymbol{\theta}_{ij}^{u} \quad \forall (i,j) \in E \tag{6d}$$

$$p_{ij}^2 + q_{ij}^2 \leqslant \boldsymbol{s}_{ij}^{u} \quad \forall (i,j) \in E \tag{6e}$$

where $\boldsymbol{s}_{ij}^u$ denotes the thermal capacity of line (i,j), $\boldsymbol{\theta}_{ij}^l$ and $\boldsymbol{\theta}_{ij}^u$ bound the phase angle difference between connected buses, and $\boldsymbol{v}_i^l, \boldsymbol{v}_i^u$ represent the lower and upper bounds on voltage magnitude at bus i. The goal is to minimize the generation cost for a set of generators G while satisfying the defined above network constraints:

$$\min \sum_{i \in G} \boldsymbol{c}_i^0 (p_i^g)^2 + \boldsymbol{c}_i^1 (p_i^g)$$

$$\text{s.t.} (4), (5), (6)$$

4.2. The Optimal Transmission Switching (OTS) Problem.

4.2.1. Previous Work on Optimal Transmission Switching. By changing the topology of a power network, congestion created by thermal limits or voltage bounds can be reduced [26, 27]. More recently, it has been observed that topology design may lead to cost savings around 10% in locational marginal price energy markets [12, 13, 17, 18, 25]. Topology design for reducing generation costs was originally suggested in [24] and formalized in [12], and is referred to as Optimal Transmissions Switching. From a mathematical standpoint, the OTS problem presents a challenging non-convex Mixed-Integer NonLinear Program (MINLP). To tackle this problem, many studies [2–4, 12, 13, 16–18] approximate the non-convex power flow equations with a linear power flow model known as the DC model. However, recent studies [9] show that the latter does not appear to be appropriate for OTS studies as it exhibits significant feasibility issues with respect to the original nonlinear model. Moreover, the approximate linear formulation can either underestimate or overestimate the benefits of line switching in different contexts.

4.2.2. Problem Definition. The OTS problem is an extension of the OPF problem where line switching is permitted. For each line (i,j) a binary variable z_{ij} indicating the status of the line is added to the model. If a line (i,j) is disconnected ($z_{ij} = 0$), then no active and reactive power can be flowing through it. This leads to disjunctive versions of constraints (4), (6d) and (6e):

$$p_{ij} = \mathbf{g}_{ij} v_i^2 - \mathbf{g}_{ij} v_i v_j \cos(\theta_{ij}) - \mathbf{b}_{ij} v_i v_j \sin(\theta_{ij}), \quad \text{if } z_{ij} = 1 \ \ \forall (i,j) \in E, \tag{7}$$

$$q_{ij} = -\mathbf{b}_{ij} v_i^2 + \mathbf{b}_{ij} v_i v_j \cos(\theta_{ij}) - \mathbf{g}_{ij} v_i v_j \sin(\theta_{ij}), \quad \text{if } z_{ij} = 1 \ \ \forall (i,j) \in E, \tag{8}$$

$$p_{ij}^2 + q_{ij}^2 \leqslant \boldsymbol{s}_{ij}^u, \quad \text{if } z_{ij} = 1 \ \ \forall (i,j) \in E, \tag{9}$$

$$p_{ij} = q_{ij} = 0, \quad \text{if } z_{ij} = 0 \ \ \forall (i,j) \in E, \tag{10}$$

$$\boldsymbol{\theta}_{ij}^l \leqslant \theta_{ij} \leqslant \boldsymbol{\theta}_{ij}^u, \quad \text{if } z_{ij} = 1 \ \ \forall (i,j) \in E, \tag{11}$$

$$\boldsymbol{M}_l \leqslant \theta_{ij} \leqslant \boldsymbol{M}_u, \quad \text{if } z_{ij} = 0 \ \ \forall (i,j) \in E, \tag{12}$$

where $\boldsymbol{M}_l$ and $\boldsymbol{M}_u$ are big-M constants guaranteeing that the variable θ_{ij} is free whenever $z_{ij} = 0$. The standard values used for $\boldsymbol{M}_l$ and $\boldsymbol{M}_u$ are given below,

$$\boldsymbol{M}_l = \sum_{E} \boldsymbol{\theta}^l_{ij} \text{ and } \boldsymbol{M}_u = \sum_{E} \boldsymbol{\theta}^u_{ij}$$

4.3. Tightening the big-M constants.

PROPOSITION 7. *Let E^u (resp. E^l) denote the set of $|N| - 1$ edges having the largest upper (resp. smallest lower) bound on the phase angle difference θ_{ij}. Then,*

$$\theta_i - \theta_j \leqslant \sum_{E^u} \boldsymbol{\theta}^u_{ij}, \text{ and } \theta_i - \theta_j \geqslant \sum_{E^l} \boldsymbol{\theta}^l_{ij}, \ \forall (i,j) \in E.$$

Proof. Due to Kirchhoff's Voltage Law, the voltage drop around a loop is zero. Observe that the longest loop-less path has at most $|N| - 1$ edges. Hence the voltage drop $\theta_i - \theta_j$ cannot be larger than the sum of the largest ($|N| - 1$) $\boldsymbol{\theta}^u_{ij}$ values. A similar argument holds for the lower bound.

∎

4.4. The Quadratic Convex (QC) Relaxation. Due to the non-convex nature of trigonometric and multilinear functions, optimality guarantees can only be provided using convex relaxations. Hijazi et al. [20] have introduced a quadratic relaxation that exploits the tight bounds on the phase angle and voltage magnitude variables θ_{ij} and v_i.

Let

$$w^R_{ij} = v_i v_j \cos(\theta_{ij}) \tag{13}$$

$$w^I_{ij} = v_i v_j \sin(\theta_{ij}) \tag{14}$$

$$w_i = v_i^2 \tag{15}$$

Using these auxiliary variables, equations (4) become linear:

$$p_{ij} = \boldsymbol{g}_{ij} w_i - \boldsymbol{g}_{ij} w^R_{ij} - \boldsymbol{b}_{ij} w^I_{ij} \tag{16}$$

$$q_{ij} = -\boldsymbol{b}_{ij} w_i + \boldsymbol{b}_{ij} w^R_{ij} - \boldsymbol{g}_{ij} w^I_{ij} \tag{17}$$

The QC relaxation [20] uses quadratic and polyhedral relaxations for $\sin(\theta_{ij})$ and $\cos(\theta_{ij})$ in conjunction with McCormick envelopes for multilinear terms. The quadratic relaxations introduced in [20] for $\cos(\theta_{ij})$ does not support asymmetrical phase angle bounds. Furthermore the on/off version of these quadratic constraints are formulated using weak big-M approaches. In light of the results presented in previous sections, we are able to improve the QC relaxation using asymmetrical quadratic relaxations and tight on/off constraints representation. As a showcase, we present below the formulation of the on/off version corresponding to the quadratic relaxation of $\sin(\theta_{ij})$ when $\boldsymbol{\theta}^u_{ij} \leqslant 0$. Similar constraints can be generated for the other cases. Let $Q^{\sin}_{ij}$ denote the auxiliary variable used in the quadratic relaxation corresponding to $\sin(\theta_{ij})$, we have,

$$\left\{\begin{array}{l} Q^{\sin}_{ij} \geqslant \boldsymbol{a}_{ij}\theta^2_{ij} + \boldsymbol{b}_{ij}\theta_{ij} + \boldsymbol{c}_{ij}, \\ \sin(\boldsymbol{\theta}^l_{ij}) \leqslant Q^{\sin}_{ij} \leqslant \sin(\boldsymbol{\theta}^u_{ij}), \\ \boldsymbol{\theta}^l_{ij} \leqslant \theta_{ij} \leqslant \boldsymbol{\theta}^u_{ij}, \\ z_{ij} = 1 \end{array}\right\} \vee \left\{\begin{array}{l} Q^{\sin}_{ij} = 0, \\ \sum_{E^l} \boldsymbol{\theta}^l_{ij} \leqslant \theta_{ij} \leqslant \sum_{E^u} \boldsymbol{\theta}^u_{ij}, \\ z_{ij} = 0 \end{array}\right\}$$

Based on Theorem 4, we can write the convex hull formulation of this disjunction as follows,

$$\begin{cases} \theta_{ij} - \sum\limits_{E^u} \boldsymbol{\theta}^u_{ij}(1-z) + \boldsymbol{\rho} z \leqslant \sqrt{\frac{Q^{\sin}_{ij} z + \delta z^2}{\boldsymbol{a}}}, \\ \theta_{ij} - \sum\limits_{E^l} \boldsymbol{\theta}^l_{ij}(1-z) + \boldsymbol{\rho} z \geqslant -\sqrt{\frac{Q^{\sin}_{ij} z + \boldsymbol{\delta} z^2}{\boldsymbol{a}}}, \\ \boldsymbol{\theta}^u_{ij} + \boldsymbol{\rho} z \geqslant -\sqrt{\frac{Q^{\sin}_{ij} z + \boldsymbol{\delta} z^2}{\boldsymbol{a}}}, \\ \boldsymbol{\theta}^l_{ij} + \boldsymbol{\rho} z \leqslant \sqrt{\frac{Q^{\sin}_{ij} z + \boldsymbol{\delta} z^2}{\boldsymbol{a}}}, \end{cases} \tag{18}$$

Note that this formulation is non-differentiable at points where $\hat{cs}_{ij} = z_{ij}$. Numerical issues arising from this irregularity can be alleviated using a linear outer approximation of the nonlinear constraints. This results in a relaxation which is still valid as the functions are convex.

4.5. On/Off Lifted Nonlinear Cuts. In this subsection, we use an alternate representation of the voltage angle bounds. Specifically, given $-\boldsymbol{\pi}/2 \leqslant \boldsymbol{\theta}^l_{ij} < \boldsymbol{\theta}^u_{ij} \leqslant \boldsymbol{\pi}/2$, we define the following constants:

$$\boldsymbol{\phi}_{ij} = (\boldsymbol{\theta}^u_{ij} + \boldsymbol{\theta}^l_{ij})/2 \tag{19a}$$

$$\boldsymbol{\delta}_{ij} = (\boldsymbol{\theta}^u_{ij} - \boldsymbol{\theta}^l_{ij})/2 \tag{19b}$$

$$\boldsymbol{v}^{\boldsymbol{\sigma}}_i = \boldsymbol{v}^{\boldsymbol{l}}_i + \boldsymbol{v}^{\boldsymbol{u}}_i \tag{19c}$$

$$\boldsymbol{v}^{\boldsymbol{\sigma}}_j = \boldsymbol{v}^{\boldsymbol{l}}_j + \boldsymbol{v}^{\boldsymbol{u}}_j \tag{19d}$$

Using the ϕ, δ, v^σ representation, now we can write the Lifted Nonlinear Cuts for the QC-OTS model. The derivation of these cuts can be found in [11].

$$\begin{aligned} &\boldsymbol{v}^{\boldsymbol{\sigma}}_i \boldsymbol{v}^{\boldsymbol{\sigma}}_j (w^R_{ij}\cos(\boldsymbol{\phi}_{ij}) + w^I_{ij}\sin(\boldsymbol{\phi}_{ij})) - \boldsymbol{v}^{\boldsymbol{u}}_j \cos(\boldsymbol{\delta}_{ij}) \boldsymbol{v}^{\boldsymbol{\sigma}}_j w_i - \\ &\boldsymbol{v}^{\boldsymbol{u}}_i \cos(\boldsymbol{\delta}_{ij}) \boldsymbol{v}^{\boldsymbol{\sigma}}_i w_j \geqslant \boldsymbol{v}^{\boldsymbol{u}}_i \boldsymbol{v}^{\boldsymbol{u}}_j \cos(\boldsymbol{\delta}_{ij})(\boldsymbol{v}^{\boldsymbol{l}}_i \boldsymbol{v}^{\boldsymbol{l}}_j - \boldsymbol{v}^{\boldsymbol{u}}_i \boldsymbol{v}^{\boldsymbol{u}}_j) \quad \forall (i,j) \in E \end{aligned} \tag{20a}$$

$$\begin{aligned} &\boldsymbol{v}^{\boldsymbol{\sigma}}_i \boldsymbol{v}^{\boldsymbol{\sigma}}_j (w^R_{ij}\cos(\boldsymbol{\phi}_{ij}) + w^I_{ij}\sin(\boldsymbol{\phi}_{ij})) - \boldsymbol{v}^{\boldsymbol{l}}_j \cos(\boldsymbol{\delta}_{ij}) \boldsymbol{v}^{\boldsymbol{\sigma}}_j w_i - \\ &\boldsymbol{v}^{\boldsymbol{l}}_i \cos(\boldsymbol{\delta}_{ij}) \boldsymbol{v}^{\boldsymbol{\sigma}}_i w_j \geqslant -\boldsymbol{v}^{\boldsymbol{l}}_i \boldsymbol{v}^{\boldsymbol{l}}_j \cos(\boldsymbol{\delta}_{ij})(\boldsymbol{v}^{\boldsymbol{l}}_i \boldsymbol{v}^{\boldsymbol{l}}_j - \boldsymbol{v}^{\boldsymbol{u}}_i \boldsymbol{v}^{\boldsymbol{u}}_j) \quad \forall (i,j) \in E \end{aligned} \tag{20b}$$

We use the convex hull formulation introduced in [19] to get a disjunctive version of these cuts.

4.6. Bounds Propagation. The strength of the QC relaxation depends on the bounds on voltage magnitudes and phase angle differences. In order to exploit this feature we apply bound propagation to the QC-OTS model, as was first proposed in [10] for the QC relaxation of the continuous Optimal Power Flow model.

For this purpose the traditional constraint-programming notions, such as minimal continuous constraint networks (CCNs) and bound-consistency, are adapted in [10] to relaxations by defining the concept of a continuous constraint relaxation network (CCRN). Algorithms for computing minimal and bound-consistent CCRNs are introduced.

In this paper we use minimal CCRNs, because they yield tighter bounds than bound-consistent networks. In [10] the minCCRN algorithm was used to propagate the bounds on θ_{ij} and v_i in the continuous QC model. To avoid solving many mixed-integer programs, in the revised minCCRN algorithm we find solutions of the continuous relaxations of the original programs. Bound propagation on the binary variables

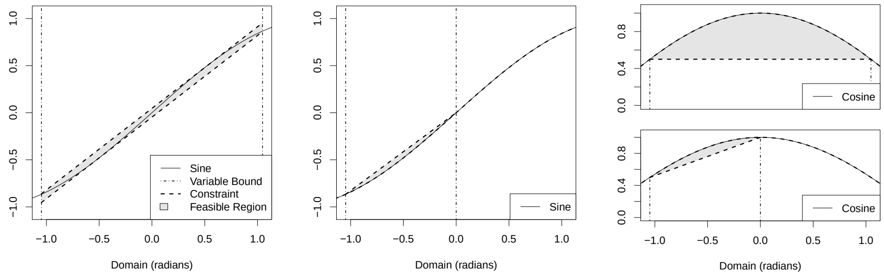

Fig. 4: The impact of variable bounds on the convex relaxations

is introduced: if the lower bound of z_{ij} in the relaxed model is proven to be greater than 0, then this variable can be fixed to 1.

5. Computational results.

5.1. Bound Propagation Strength and Performance. This section evaluates the bound propagation algorithm on 28 test cases from the NICTA Energy Systems Test Case Archive (NESTA) - v0.5.0 [8] ranging from 3 to 300 nodes. The models were implemented in C++ and solved using Gurobi 6.5.0 on Dell PowerEdge 1950 machines with 2x 2.00GHz Intel Quad Core Xeon E5405 CPUs and 16GB of memory.

In our experiments, we only select instances where the original QC-OTS model provides an optimality gap greater than 1%. The optimality gap is calculated as the relative difference between the upper bound obtained from solving the exact AC-OTS model and the lower bound returned by the QC relaxations of the OTS model. Upper bounds on the solution of the non-convex AC-OTS model were computed using Bonmin-1.8.4.

Table 1 summarizes the bound propagation results using the following metrics: sequential runtime of the algorithm, parallel runtime, reduction in the size of θ and v domains after bound propagation (measured in percentage of the the original domain size) and number of free lines, i.e. lines where z cannot be fixed to 1 or 0 after bound propagation (measured in percentage of the total number of lines in the network).

5.2. Results on the QC-OTS models. This subsection discusses the results on the QC-OTS models. The computational environment is the same as in the previous subsection. The convergence tolerance on the relative difference between upper and lower bounds on the solutions of mixed-integer problems was set to $\epsilon = 0.01$, and the time limit was set to 7200 seconds.

We present the results for the following modifications of the QC-OTS model:

- S - simple QC-OTS model without any improvements.
- BP - model with bound propagation.
- Qtrig - model with bound propagation and improved quadratic relaxations of trigonometric functions.

The 'SQ' suffix indicates that the convex hull formulation was used to represent quadratic on/off constraints, while 'M' indicates the use of a big-M formulation.

Table 2 shows the runtimes in seconds. It can be seen that the new formulation improves the runtime compared to the standard big-M approach, especially in the

Table 1: Bound propagation results

Test Case	Sequential time(s)	Parallel time(s)	θ domain (%)	v domain (%)	Free lines (%)
3_lmbd	0.41	0.07	41.93	100	33.33
30_ieee	99.87	2.04	16.86	94.37	90.24
118_ieee	1572.70	8.20	34.25	98.12	97.31
162_ieee_dtc	5123.70	19.15	35.01	98.08	97.54
300_ieee	13736	27.69	38.98	10.69	80.54
3_lmbd__api	0.54	0.10	7.11	59.62	33.33
6_ww__api	5.11	0.34	1.14	19.93	45.45
24_ieee_rts__api	80.20	2.03	28.3	66.83	55.26
30_as__api	94.74	1.79	8.55	80.05	48.78
5_pjm	2.31	0.17	16.78	99.05	100.00
30_fsr__api	82.15	1.94	12.86	96.3	90.24
30_ieee__api	99.02	2.60	12.08	88.24	65.85
39_epri__api	140.45	2.78	12.66	96.21	52.17
73_ieee_rts__api	885.07	14.06	31.82	67.57	59.17
118_ieee__api	1589.64	11.38	31.6	97.38	91.94
189_edin__api	2987.68	16.08	13.46	96.01	75.24
300_ieee__api	12703	27.81	37.79	89.6	80.54
3_lmbd__sad	0.42	0.04	3.39	33.53	33.33
5_pjm__sad	1.47	0.13	17.45	45.15	33.33
24_ieee_rts__sad	47.90	1.35	64.32	92.94	68.42
29_edin__sad	255.09	5.15	95.13	98.56	97.98
30_as__sad	56.19	1.01	53.73	94.01	73.17
30_ieee__sad	77.53	1.48	38.63	90.24	82.93
73_ieee_rts__sad	537.84	5.50	69.03	94	75.83
118_ieee__sad	1289.59	6.36	72.97	97.85	94.62
162_ieee_dtc__sad	4697.00	18.50	60.7	98.07	70.39
189_edin__sad	2431.62	11.87	25.07	95.2	70.39
300_ieee__sad	10407	30.08	32.94	10.49	80.05
Average	2107.29	2.82	32.66	78.86	70.62

case of asymmetric bounds with models BP and Qtrig where we respectively observe 8% and 14% time reduction on average.

Table 3 presents the optimality gaps. Bound propagation significantly tightens the relaxations and thus improves the gap.

In Table 4, we compare the gaps yielded by the QC-OTS model and the MISOCP model [21] on NESTA - v0.3.0 instances.

Finally, Table 5 compares the original QC-OTS model with the strengthened model which includes all improvements introduced in this paper. Observe that on 10 instances out of 28, the new formulation reduces the optimality gap to less than 1%, thus marking them as "closed".

6. Conclusion. This work introduces an explicit formulation of one-dimensional quadratic disjunctive constraints. The new formulation leads to tighter continuous relaxations when compared to the standard big-M approach, all while avoiding to add new variables into the model. This result was applied to the Quadratic Convex (QC) relaxation of the Optimal Transmission Switching problem. Numerical experiments showed that the new convex hull formulation leads to an improvement in solution times. Furthermore, exploiting the new relaxations for trigonometric functions, bound propagation helped reduce the optimality gap on all test cases, closing 10 out of 28 open instances.

Table 2: Runtimes (s)

Test Case	Qtrig-SQ	Qtrig-M	BP-SQ	BP-M	S-SQ	S-M
3_lmbd	0.12	0.16	0.13	0.15	**0.05**	0.07
30_ieee	10.19	9.45	11.25	10.25	2.67	**1.36**
118_ieee	129.37	451.47	234.15	441.16	**55.8**	59
162_ieee_dtc	285.63	438.28	308.75	496.59	**243.03**	254
300_ieee	7200	7200	7200	7200	7200	7200
3_lmbd__api	0.13	0.14	0.13	0.13	0.03	**0.02**
6_ww__api	0.58	0.59	0.58	0.61	0.15	**0.14**
24_ieee_rts__api	6.35	6.18	5.49	9.82	**2.58**	2.84
30_as__api	7.09	9.34	8.47	8.79	**1.13**	1.25
5_pjm	0.4	0.39	0.40	0.43	0.12	**0.11**
30_fsr__api	6.68	7.27	6.01	6.91	5.12	**1.48**
30_ieee__api	4.07	4.79	4.04	4.60	**1.33**	1.37
39_epri__api	7.96	10.53	8.60	9.44	4.48	**0.03**
73_ieee_rts__api	707.51	196.91	87.09	138.13	**15.5**	53
118_ieee__api	7200	7200	7200	7200	35.39	**13.58**
189_edin__api	7200	7200	7200	7200	**395.41**	507
300_ieee__api	1214.01	7200	568.05	1435.37	**531.5**	756
3_lmbd__sad	0.08	0.08	0.08	0.08	0.04	**0.03**
5_pjm__sad	0.22	0.29	0.25	0.21	**0.07**	0.08
24_ieee_rts__sad	70.21	66.90	89.03	82.40	92.64	**69**
29_edin__sad	7200	7200	7200	7200	7200	7200
30_as__sad	11.16	11.25	14.86	12.70	**6.16**	13.12
30_ieee__sad	5.67	3.98	4.86	4.05	4.3	**2.46**
73_ieee_rts__sad	3077.75	2401.42	2047.03	2676.31	**314.88**	561
118_ieee__sad	7200	7200	7200	7200	7200	7200
162_ieee_dtc__sad	7200	7200	1172.38	7200	**381.96**	613
189sad	**251.92**	450.72	382.31	298.00	437.46	1366
300_ieee__sad	7200	7200	7200	7200	7200	7200
Average	2007.70	2202.51	1719.79	2001.29	**1118.99**	1181.28

Table 3: Optimality gaps (%)

Test Case	AC-OTS cost	Qtrig	BP	S
3_lmbd	5813	**1.27**	1.28	**1.27**
30_ieee	194	**3.66**	**3.66**	11.49
118_ieee	3690	**1.14**	1.36	1.39
162_ieee_dtc	4137	**2.01**	2.03	2.06
300_ieee	16895	2.85	**2.82**	2.98
3_lmbd_api	367	**0.54**	**0.54**	1.63
6_ww_api	252	**0.40**	**0.40**	6.03
24_ieee_rts_api	6055	**1.77**	1.85	7.39
30_as_api	553	**1.27**	1.45	1.86
5_pjm	15174	**1.05**	1.15	1.15
30_fsr_api	205	**0.98**	**0.98**	2.15
30_ieee_api	414	0.72	0.72	**0.71**
39_epri_api	7359	**0.49**	0.73	1.66
73_ieee_rts_api	17510	**0.49**	0.86	1.20
118_ieee_api	6018	**3.42**	3.56	4.14
189_edin_api	1947	5.19	**4.93**	5.31
300_ieee_api	22825	**0.83**	**0.83**	1.03
3_lmbd_sad	5990	**0.03**	**0.03**	1.20
5_pjm_sad	26423	0.51	**0.14**	1.22
24_ieee_rts_sad	78346	2.23	**1.58**	4.09
29_edin_sad	38061	**18.82**	18.93	18.96
30_as_sad	907	**1.43**	**1.43**	2.32
30_ieee_sad	205	**0.98**	1.46	4.84
73_ieee_rts_sad	226046	**0.08**	1.02	1.66
118_ieee_sad	3932	**3.81**	3.97	3.97
162_ieee_dtc_sad	4147	**0.60**	2.22	2.24
189_edin_sad	906	**1.77**	2.76	2.54
300_ieee_sad	16912	**2.77**	2.78	2.93
Average		**2.18**	2.34	3.55

Table 4: Comparing results with the MISOCP model [21]

Test Case	AC-OTS cost	Gap - QC-OTS (%)	Gap - MISOCP (%)
3_lmbd_api	367	**0.62**	1.17
4_gs_api	767	0.00	0.00
5_pjm_api	2987	0.02	0.02
6_ww_api	252	**0.54**	1.05
9_wscc_api	656	0.00	0.00
14_ieee_api	321	**0.31**	0.41
29_edin_api	295160	**0.21**	0.33
30_as_api	553	**0.31**	0.34
30_ieee_api	409	0.18	**0.15**
30_fsr_api	204	0.14	**0.03**
39_epri_api	7359	**0.41**	0.70
57_ieee_api	1429	0.10	**0.09**
118_ieee_api	6018	**3.80**	7.50
162_ieee_dtc_api	6018	**0.36**	0.60
189_edin_api	1947	**3.36**	5.58
300_ieee_api	22825	1.04	**0.61**
Average		**0.73**	1.16

Table 5: Comparing the original QC-OTS model with the strengthened model including all improvements.

Test Case	Runtime (s) (original)	Runtime (s) (strengthened)	Gap (%) (original)	Gap (%) (strengthened)
3_lmbd	**0.07**	0.10	1.27	**0.24**
30_ieee	**1.36**	8.75	11.49	**2.88**
118_ieee	**59**	208.51	1.39	**1.16**
162_ieee_dtc	**254**	779.39	2.06	**2.01**
300_ieee	7200	7200	2.98	**2.85**
3_lmbd__api	**0.02**	0.12	1.63	**0.42**
6_ww__api	**0.14**	0.38	6.03	**0.01**
24_ieee_rts__api	**2.84**	6.32	7.39	**1.56**
30_as__api	**1.25**	7.80	1.86	**1.25**
5_pjm	**0.11**	0.29	1.15	**1.14**
30_fsr__api	**1.48**	6.24	2.15	**0.63**
30_ieee__api	**1.37**	5.56	0.71	**0.36**
39_epri__api	**0.03**	9.19	1.66	**0.42**
73_ieee_rts__api	**53**	94.93	1.20	**0.25**
118_ieee__api	**13.58**	7200	4.14	**3.28**
189_edin__api	**507**	7200	5.31	**4.94**
300_ieee__api	**756**	7200	1.03	**0.83**
3_lmbd__sad	**0.03**	0.12	1.20	**0.00**
5_pjm__sad	**0.08**	0.19	1.22	**0.98**
24_ieee_rts__sad	69	**65.63**	4.09	**2.21**
29_edin__sad	7200	7200	18.96	**18.57**
30_as__sad	13.12	**8.48**	2.32	**1.34**
30_ieee__sad	**2.46**	5.85	4.84	**1.20**
73_ieee_rts__sad	**561**	2518.75	1.66	**0.87**
118_ieee__sad	7200	7200	3.97	**3.81**
162_ieee_dtc__sad	**613**	7200	2.24	**2.20**
189sad	1366	**274.54**	2.54	**1.77**
300_ieee__sad	7200	7200	2.93	**2.77**
Average	**1181.28**	2205.15	3.55	**2.18**

REFERENCES

[1] E. Balas, S. Ceria, and G. Cornuéjols, *A lift-and-project cutting plane algorithm for mixed 0–1 programs*, Mathematical programming, 58 (1993), pp. 295–324.

[2] C. Barrows and S. Blumsack, *Transmission switching in the rts-96 test system*, IEEE Transactions on Power Systems, 27 (2012), pp. 1134–1135, http://dx.doi.org/10.1109/TPWRS.2011.2170771.

[3] C. Barrows, S. Blumsack, and R. Bent, *Computationally efficient optimal transmission switching: Solution space reduction*, in Power and Energy Society General Meeting, 2012

IEEE, July 2012, pp. 1–8, http://dx.doi.org/10.1109/PESGM.2012.6345550.

[4] C. Barrows, S. Blumsack, and P. Hines, *Correcting optimal transmission switching for ac power flows*, in System Sciences (HICSS), 2014 47th Hawaii International Conference on, Jan 2014, pp. 2374–2379.

[5] P. Belotti, P. Bonami, M. Fischetti, A. Lodi, M. Monaci, A. Nogales-Gómez, and D. Salvagnin, *On handling indicator constraints in mixed integer programming*, Computational Optimization and Applications, (2016), pp. 1–22, http://dx.doi.org/10.1007/s10589-016-9847-8, http://dx.doi.org/10.1007/s10589-016-9847-8.

[6] P. Bonami, A. Lodi, A. Tramontani, and S. Wiese, *On mathematical programming with indicator constraints*, Mathematical Programming, 151 (2015), pp. 191–223, http://dx.doi.org/10.1007/s10107-015-0891-4, http://dx.doi.org/10.1007/s10107-015-0891-4.

[7] S. Ceria and J. Soares, *Convex programming for disjunctive convex optimization*, Mathematical Programming, 86 (1999), pp. 595–614, http://dx.doi.org/10.1007/s101070050106.

[8] C. Coffrin, D. Gordon, and P. Scott, *NESTA, The* NICTA *Energy System Test Case Archive*, CoRR, abs/1411.0359 (2014), http://arxiv.org/abs/1411.0359.

[9] C. Coffrin, H. Hijazi, K. Lehmann, and P. Van Hentenryck, *Primal and dual bounds for optimal transmission switching*, Power Systems Computation Conference (PSCC), (2014), pp. 1–8, http://dx.doi.org/10.1109/PSCC.2014.7038446.

[10] C. Coffrin, H. Hijazi, and P. Van Hentenryck, *Strengthening convex relaxations with bound tightening for power network optimization*, in Principles and Practice of Constraint Programming, G. Pesant, ed., vol. 9255 of Lecture Notes in Computer Science, Springer International Publishing, 2015, pp. 39–57, http://dx.doi.org/10.1007/978-3-319-23219-5_4, http://dx.doi.org/10.1007/978-3-319-23219-5_4.

[11] C. Coffrin, H. L. Hijazi, and P. V. Hentenryck, *Strengthening the SDP Relaxation of AC Power Flows with Convex Envelopes, Bound Tightening, and Lifted Nonlinear Cuts*, CoRR, abs/1512.04644 (2015), http://arxiv.org/abs/1512.04644.

[12] E. Fisher, R. O'Neill, and M. Ferris, *Optimal transmission switching*, IEEE Transactions on Power Systems, 23 (2008), pp. 1346–1355, http://dx.doi.org/10.1109/TPWRS.2008.922256.

[13] J. Fuller, R. Ramasra, and A. Cha, *Fast heuristics for transmission-line switching*, IEEE Transactions on Power Systems, 27 (2012), pp. 1377–1386, http://dx.doi.org/10.1109/TPWRS.2012.2186155.

[14] I. E. Grossmann and S. Lee, *Generalized convex disjunctive programming: Nonlinear convex hull relaxation*, Computational Optimization and Applications, 26, pp. 83–100, http://dx.doi.org/10.1023/A:1025154322278, http://dx.doi.org/10.1023/A:1025154322278.

[15] O. Günlük and J. Linderoth, *Perspective reformulations of mixed integer nonlinear programs with indicator variables*, Mathematical Programming, 124 (2010), pp. 183–205.

[16] K. Hedman, M. Ferris, R. O'Neill, E. Fisher, and S. Oren, *Co-optimization of generation unit commitment and transmission switching with n-1 reliability*, in Power and Energy Society General Meeting, 2010 IEEE, July 2010, pp. 1–1, http://dx.doi.org/10.1109/PES.2010.5589434.

[17] K. Hedman, R. O'Neill, E. Fisher, and S. Oren, *Optimal transmission switching — sensitivity analysis and extensions*, IEEE Transactions on Power Systems, 23 (2008), pp. 1469–1479, http://dx.doi.org/10.1109/TPWRS.2008.926411.

[18] K. Hedman, R. O'Neill, E. Fisher, and S. Oren, *Optimal transmission switching with contingency analysis*, IEEE Transactions on Power Systems, 24 (2009), pp. 1577–1586.

[19] H. Hijazi, P. Bonami, G. Cornujols, and A. Ouorou, *Mixed-integer nonlinear programs featuring on/off constraints*, Computational Optimization and Applications, 52 (2012), pp. 537–558.

[20] H. Hijazi, C. Coffrin, and P. Van Hentenryck, *Convex quadratic relaxations of mixed-integer nonlinear programs in power systems.* Published online at http://www.optimization-online.org/DB_HTML/2013/09/4057.html, 2013.

[21] B. Kocuk, S. S. Dey, and X. A. Sun, *New Formulation and Strong MISOCP Relaxations for AC Optimal Transmission Switching Problem*, ArXiv e-prints, (2015), arXiv:1510.02064.

[22] L. Lovász and A. Schrijver, *Cones of matrices and set-functions and 0-1 optimization*, SIAM Journal on Optimization, 1 (1991), pp. 166–190.

[23] G. Nemhauser and L. Wolsey, *Integer and combinatorial optimization*, Wiley-Interscience series in discrete mathematics and optimization, 1988.

[24] R. O'Neill, R. Baldick, U. Helman, M. Rothkopf, and J. Stewart, W., *Dispatchable transmission in rto markets*, IEEE Transactions on Power Systems, 20 (2005), pp. 171–179, http://dx.doi.org/10.1109/TPWRS.2004.841168.

[25] T. Potluri and K. Hedman, *Impacts of topology control on the acopf*, in Power and Energy

Society General Meeting, 2012 IEEE, 2012, pp. 1–7, http://dx.doi.org/10.1109/PESGM.2012.6345676.

[26] J. Rolim and L. Machado, *A study of the use of corrective switching in transmission systems*, IEEE Transactions on Power Systems, 14 (1999), pp. 336–341, http://dx.doi.org/10.1109/59.744552.

[27] W. Shao and V. Vittal, *Corrective switching algorithm for relieving overloads and voltage violations*, IEEE Transactions on Power Systems, 20 (2005), pp. 1877–1885, http://dx.doi.org/10.1109/TPWRS.2005.857931.

[28] H. D. Sherali and W. P. Adams, *A hierarchy of relaxations between the continuous and convex hull representations for zero-one programming problems*, SIAM Journal on Discrete Mathematics, 3 (1990), pp. 411–430.

[29] A. R. Stubbs and S. Mehrotra, *A branch-and-cut method for 0-1 mixed convex programming*, Mathematical Programming, 86, pp. 515–532, http://dx.doi.org/10.1007/s101070050103, http://dx.doi.org/10.1007/s101070050103.